

## Raman Spectroelectrochemistry of Molecules within Individual Electromagnetic Hot Spots

Timur Shegai,<sup>†,§</sup> Alexander Vaskevich,<sup>‡</sup> Israel Rubinstein,<sup>‡</sup> and Gilad Haran<sup>\*,†</sup>

Department of Chemical Physics and the Department of Materials and Interfaces, Weizmann Institute of Science, 76100, Rehovot, Israel

Received June 3, 2009; E-mail: gilad.haran@weizmann.ac.il

**Abstract:** The role of chemical enhancement in surface-enhanced Raman scattering (SERS) remains a contested subject. We study SERS spectra of 4-mercaptopyridine molecules excited far from the molecular resonance, which are collected from individual electromagnetic hot spots at concentrations close to the single-molecule limit. The hot spots are created by depositing Tollen's silver island films on a transparent electrode incorporated within an electrochemical cell. Analysis of the intensity of the spectra relative to those obtained from individual rhodamine 6G molecules on the same surface provides a lower limit of  $\sim 3$  orders of magnitude for the chemical enhancement. This large enhancement is likely to be due to a charge transfer resonance involving the transfer of an electron from the metal to an adsorbed molecule. Excitation at three different wavelengths, as well as variation of electrode potential from 0 to  $-1.2$  V, lead to significant changes in the relative intensities of bands in the spectrum. It is suggested that while the bulk of the enhancement is due to an Albrecht A-term resonance Raman effect (involving the charge transfer transition), vibronic coupling provides additional enhancement which is sensitive to electrode potential. The measurement of potential-dependent SERS spectra from individual hot spots opens the way to a thorough characterization of chemical enhancement, as well to studies of redox phenomena at the single-molecule level.

### Introduction

Surface-enhanced Raman scattering (SERS) has gained renewed interest following the discovery that it is possible to observe spectra from single molecules.<sup>1–3</sup> It is generally agreed that there are two contributions to the SERS enhancement, electromagnetic (EM) and chemical. The dominant EM enhancement occurs due to collective oscillations of surface electrons in metal nanoparticles, leading to a local field which is much stronger than the incident field. The strength of the local field is manifested in significant amplification of the otherwise weak Raman scattering. The cross section of SERS is roughly proportional to the fourth power of the local electric field because both incident and scattered fields get coupled to the plasmon resonance.<sup>4</sup> The distribution of the enhancement over even quite simple nanoparticle arrangements is rather heterogeneous.<sup>5,6</sup> A particularly strong enhancement is achieved in narrow junctions between closely spaced nanoparticles (“hot spots”), where the EM enhancement factor can reach values of

$10^{10}$ – $10^{11}$ .<sup>7,8</sup> This is probably the strongest enhancement predicted for realistic arrangements of metal nanoparticles. However, even such a strong response cannot guarantee single-molecule sensitivity unless an additional mechanism is involved. Further enhancement can be provided by the molecular resonant Raman effect. For example, the Raman scattering cross section of the commonly used dye rhodamine-6G (R6G) is enhanced by  $\sim 6$  orders of magnitude when it is resonantly excited,<sup>9,10</sup> which together with EM enhancement in a hot spot can impart single-molecule sensitivity.

Additional enhancement of the Raman signal of surface-adsorbed molecules is attributed to the so-called “chemical mechanism”, which is still not completely understood, and is therefore the subject of ongoing research.<sup>11</sup> Over the years several groups have attempted to separate the contribution from the chemical enhancement from that of the EM enhancement. For example, in work by Campion and co-workers,<sup>12,13</sup> SERS signals were registered from molecules adsorbed on smooth metal surfaces, which were unable to couple to the electromagnetic field of the excitation light and enhance it. Thus, all

<sup>†</sup> Department of Chemical Physics.

<sup>‡</sup> Department of Materials and Interfaces.

<sup>§</sup> Current address: Department of Applied Physics – Bionanophotonics, Chalmers University of Technology, SE-412 96 Goteborg, Sweden.

(1) Nie, S. M.; Emory, S. R. *Science* **1997**, *275*, 1102–1106.

(2) Kneipp, K.; Wang, Y.; Kneipp, H.; Perelman, L. T.; Itzkan, I.; Dasari, R.; Feld, M. S. *Phys. Rev. Lett.* **1997**, *78*, 1667–1670.

(3) Le Ru, E. C.; Meyer, M.; Etchegoin, P. G. *J. Phys. Chem. B* **2006**, *110*, 1944–1948.

(4) Moskovits, M. *Rev. Mod. Phys.* **1985**, *57*, 783–826.

(5) Fang, Y.; Seong, N. H.; Dlott, D. D. *Science* **2008**, *321*, 388–392.

(6) Le Ru, E. C.; Etchegoin, P. G.; Meyer, M. *J. Chem. Phys.* **2006**, *125*, 204701.

(7) Xu, H. X.; Aizpurua, J.; Kall, M.; Apell, P. *Phys. Rev. E* **2000**, *62*, 4318–4324.

(8) Li, K. R.; Stockman, M. I.; Bergman, D. J. *Phys. Rev. Lett.* **2003**, *91*, 227402.

(9) Shim, S.; Stuart, C. M.; Mathies, R. A. *ChemPhysChem* **2008**, *9*, 697–699.

(10) Jensen, L.; Schatz, G. C. *J. Phys. Chem. A* **2006**, *110*, 5973–5977.

(11) Lombardi, J. R.; Birke, R. L. *J. Phys. Chem. C* **2008**, *112*, 5605–5617.

(12) Campion, A.; Ivanecy, J. E.; Child, C. M.; Foster, M. *J. Am. Chem. Soc.* **1995**, *117*, 11807–11808.

(13) Campion, A.; Kambhampati, P. *Chem. Soc. Rev.* **1998**, *27*, 241–250.

observed enhancement could be attributed to a chemical mechanism, which was found in this work to contribute a factor of  $\sim 30$ . Peyser-Capadona et al.<sup>14</sup> reported single-molecule SERS from molecules attached to atomic clusters of silver, which are unable to support collective plasma oscillations. The enormous enhancement sustained by the silver clusters was therefore attributed to a chemical mechanism, probably due to intensity borrowing from the electronic transitions of the clusters themselves. Hu et al.<sup>15</sup> reported a  $10^8$  enhancement factor for the  $9b_2$  mode of 4-aminothiophenol sandwiched between gold and silver nanoparticles and excited far from either plasmon or molecular resonance and attributed at least part of this enhancement to a chemical effect.

From the examples given here, it becomes clear that the magnitude of the chemical enhancement varies from publication to publication and from molecule to molecule, depending on experimental conditions. The situation is even more complicated when the chemical enhancement accompanies significant EM enhancement, in which case it becomes exceedingly difficult to estimate the magnitude of each mechanism.

Uncertainty with respect to the magnitude of the chemical enhancement notwithstanding, at least two different effects were proposed to account for this process. First, it has been noted that ground-state charge transfer between the molecule and the metal can change the polarizability of the molecule, thereby affecting its Raman scattering cross section.<sup>16–18</sup> Second, it was suggested that the interaction between the adsorbed molecule and the surface is reflected in the appearance of a new electronic excitation channel, in this case via a photoinduced charge transfer (CT) mechanism.<sup>11,19–22</sup> In this so-called CT resonance model the transition energy depends on the energy separation between metallic and molecular levels. Thus, tuning the excitation energy (using a tunable laser source), or alternatively the position of the Fermi level of the metal (using an external voltage source), can in principle drive the entire system in and out of the CT resonance.

The latter approach was extensively employed in the past to study the CT resonance contribution, e.g. by examining the dependence of SERS spectra of pyridine and other benzene derivatives on electrochemical potential.<sup>20,23–27</sup> The results indicated that the SERS intensity indeed shows a resonance-like behavior dependent on the applied potential. In these ‘bulk’ experiments, which were typically carried out on roughened

electrodes, many hot spots as well as areas with more modest enhancement contributed to the total Raman signal. Quantifying the contribution of various mechanisms to the SERS intensity in such experiments requires knowledge of the hot-spot distribution, the molecular orientation, and the coverage on the highly heterogeneous surface, information which is practically unattainable. In addition, molecules like pyridine and pyrazine are adsorbed weakly (physisorbed) on the surface, and this mode of adsorption might lead to potential-dependent molecular coverage effects, thereby affecting the Raman intensity.

It should be noted that the interpretation of potential-induced changes in SERS intensities in terms of a CT mechanism was disputed in some cases, and an alternative explanation, evoking reorientation of adsorbed molecules on the metal surface, was offered. Indeed, potential-dependent changes in molecular equilibrium orientation were either demonstrated directly by using scanning tunneling microscopy (STM)<sup>28</sup> or deduced from SERS spectra using surface selection rules.<sup>27,29,30</sup>

The discussion above demonstrates the complexity associated with studies of chemical enhancement in SERS. In the work reported here we attempt to overcome part of this complexity by collecting SERS signals from just one hot spot at a time under electrochemical conditions. As a substrate we use silver islands deposited on an indium tin oxide (ITO) electrode. As a target molecule we use the relatively simple,  $C_{2v}$  symmetric 4-mercapto-pyridine (4MPy). The choice of this molecule is directed by its strong chemical binding to silver via the sulfhydryl group and its well-defined symmetry which facilitates reorientation analysis. Single-molecule Raman spectroscopy of 4MPy was demonstrated by Rothberg and co-workers.<sup>31,32</sup>

The current study has two aims. First, we attempt to estimate the *magnitude* of the chemical enhancement of 4MPy molecules, using R6G as a reference. Second, we investigate the *mechanism* of chemical enhancement by probing the potential-dependent response of these molecules under electrochemical conditions. We use several excitation energies (488, 532, and 633 nm) to discriminate between the CT mechanism and potential-induced molecular reorientation. The latter process is dictated by the surface selection rules and consequently should be excitation independent, while the former is defined by the match between the incoming photon energy and the CT transition energy.<sup>23–25</sup>

## Methods

Silver islands were prepared directly on an ITO-covered glass coverslip using Tollens’ “mirror reaction”, which involves chemical reduction of silver nitrate with glucose under basic conditions.<sup>33</sup> In particular, 10  $\mu\text{L}$  of a 0.8 M KOH solution were added to 80  $\mu\text{L}$  of a solution containing 25 mM  $\text{AgNO}_3$  and 50 mM  $\text{NH}_3(\text{aq})$ . A brown-black precipitate of  $\text{Ag}_2\text{O}$  was formed. 20  $\mu\text{L}$  of a 0.2 M  $\text{NH}_3(\text{aq})$  solution were then added, and the solution was stirred until the precipitate completely dissolved (sometimes a bit more of the ammonia solution was added to reach complete dissolution). Finally, 100  $\mu\text{L}$  of a 0.2 M glucose solution in water were added, resulting in an almost immediate change of color from transparent to yellow and then to yellow-brown due to formation of silver nanoparticles.

- (14) Peyser-Capadona, L.; Zheng, J.; Gonzalez, J. I.; Lee, T. H.; Patel, S. A.; Dickson, R. M. *Phys. Rev. Lett.* **2005**, *94*, 058301.
- (15) Hu, X. G.; Wang, T.; Wang, L.; Dong, S. J. *J. Phys. Chem. C* **2007**, *111*, 6962–6969.
- (16) Zhao, L. L.; Jensen, L.; Schatz, G. C. *J. Am. Chem. Soc.* **2006**, *128*, 2911–2919.
- (17) Zhao, L. L.; Jensen, L.; Schatz, G. C. *Nano Lett.* **2006**, *6*, 1229–1234.
- (18) Sun, M. T.; Wan, B. S.; Liu, Y. J.; Jia, Y.; Xu, H. X. *J. Raman Spectrosc.* **2008**, *39*, 402–408.
- (19) Avouris, P.; Demuth, J. E. *J. Chem. Phys.* **1981**, *75*, 4783–4794.
- (20) Arenas, J. F.; Woolley, M. S.; Otero, J. C.; Marcos, J. I. *J. Phys. Chem.* **1996**, *100*, 3199–3206.
- (21) Lombardi, J. R.; Birke, R. L.; Lu, T.; Xu, J. *J. Chem. Phys.* **1986**, *84*, 4174–4180.
- (22) Otto, A. *J. Raman Spectrosc.* **2005**, *36*, 497–509.
- (23) Billmann, J.; Otto, A. *Solid State Commun.* **1982**, *44*, 105–107.
- (24) Furtak, T. E.; Macomber, S. H. *Chem. Phys. Lett.* **1983**, *95*, 328–332.
- (25) Osawa, M.; Matsuda, N.; Yoshii, K.; Uchida, I. *J. Phys. Chem.* **1994**, *98*, 12702–12707.
- (26) Arenas, J. F.; Woolley, M. S.; Tocon, I. L.; Otero, J. C.; Marcos, J. I. *J. Chem. Phys.* **2000**, *112*, 7669–7683.
- (27) Chao, Y. W.; Zhou, Q.; Li, Y.; Yan, Y. R.; Wu, Y.; Zheng, J. W. *J. Phys. Chem. C* **2007**, *111*, 16990–16995.

- (28) Cai, W. B.; Wan, L. J.; Noda, H.; Hibino, Y.; Ataka, K.; Osawa, M. *Langmuir* **1998**, *14*, 6992–6998.
- (29) Aguiar, H. B.; Sant’Ana, A. C.; Temperini, M. L. A.; Corio, P.; Cunha, F. *Vib. Spectrosc.* **2006**, *40*, 127–132.
- (30) Wen, R.; Fang, Y. *Vib. Spectrosc.* **2005**, *39*, 106–113.
- (31) Wang, Z.; Pan, S.; Krauss, T. D.; Du, H.; Rothberg, L. J. *Proc. Natl. Acad. Sci. U.S.A.* **2003**, *100*, 8638–8643.
- (32) Wang, Z. J.; Rothberg, L. J. *J. Phys. Chem. B* **2005**, *109*, 3387–3391.
- (33) Saito, Y.; Wang, J. J.; Smith, D. A.; Batchelder, D. N. *Langmuir* **2002**, *18*, 2959–2961.

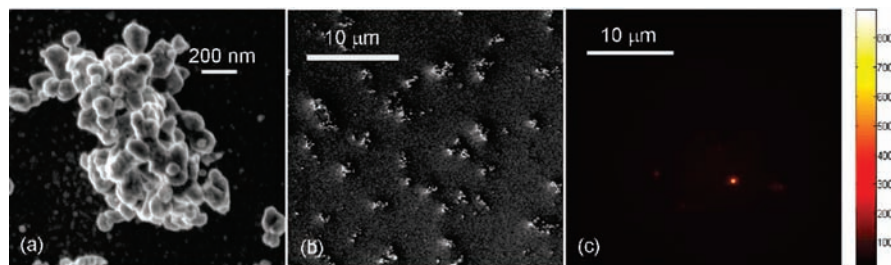


**Figure 1.** (a and b) SEM images of typical Tollens' islands adsorbed on an ITO electrode, taken at different magnifications (see the scale bars) before applying potential sweeps. The sizes of aggregates are larger than  $1 \mu\text{m}$ ; however irregularities appear on a subwavelength scale allowing intense SERS. From panel (b) one can estimate the surface area occupied by Tollens' islands. (c) Optical image of a SERS hot spot containing 4MPy molecules, obtained by excitation at 532 nm. The scale bar is the same as that in panel (b), and the illuminated area is  $\sim 10 \times 10 \mu\text{m}^2$ . The color scale on the right represents the number of counts per pixel. Note that there is only one intense spot in the image. Comparison of panels (b) and (c) suggests that the diffraction limited bright spot in panel (c) is smaller than the size of a typical cluster in panel (b).

Aggregates of silver nanoparticles formed directly on the surface of the ITO slide (Figure 1a and 1b). The reaction was typically left to proceed for 5 min, after which the surface was washed with an excess of double-distilled water and dried with a nitrogen stream.

A spectroelectrochemical cell of a three-electrode configuration, suitable for microscopic observation, was designed and built. The outer edge of a glass tube was glued by epoxy resin to the ITO slide, forming a well. A platinum wire and a silver wire covered by an AgCl layer served as the counter and reference electrodes, respectively. The latter was stored in a 0.1 M NaCl aqueous solution, the same electrolyte used in all experiments (vide infra). The electrochemical potential was measured with respect to the Ag/AgCl<sub>sat.</sub> 0.1 M NaCl reference electrode. The electrochemical accessibility of Ag islands was checked using the surface selectivity of under-potential deposition (UPD) of Pb, which proceeds exclusively on the Ag surface and not on the ITO electrode. The shape of the potentiodynamic curve (not shown) was typical for Pb UPD on a polycrystalline Ag electrode, with single peaks for deposition and dissolution of the UPD layer (see ref 34 and references therein). The areas of both peaks were identical within experimental error. Due to the influence of the Pb UPD on the morphology of Ag islands and fast morphology reshaping (vide infra), their overall surface area could not be evaluated from this measurement.

The working electrode was connected to a potentiostat (Pine Instrument Company) through a gold wire, which was glued to the ITO slide by a conductive epoxy resin outside the glass tube. The total geometric area of the working electrode exposed to the electrolyte solution was  $\sim 0.6 \text{ cm}^2$ . Counter and reference electrodes were fixed near the glass wall by a Teflon cylindrical holder, allowing observation of the central part of the working electrode surface under the microscope.  $200 \mu\text{L}$  of a 100 nM water solution of 4MPy were added on top of the working electrode, and the molecules were allowed to adsorb on the silver aggregates for 15 min.

After 4MPy adsorption the cell was washed with an excess of double distilled water to remove molecules which were not chemisorbed. The cell was then filled with 0.5 mL of a 0.1 M NaCl electrolyte solution, which was followed by one potential scan from 0 to  $-1.2 \text{ V}$  and back at a scan rate of  $9.6 \text{ mV s}^{-1}$ , to remove weakly adsorbed molecules. The cell was then washed again with an excess of double distilled water and filled with a fresh electrolyte solution.

For SERS measurements we used three different lasers, operating at 488 nm (Ar<sup>+</sup>), 532 nm (Nd: YVO<sub>4</sub>), and 633 nm (He–Ne). In all experiments and at all wavelengths the laser power was  $\sim 750 \mu\text{W}$ , and it was focused to a spot of  $\sim 10 \mu\text{m}$  in diameter by means of a long focal-length lens ( $f = 50 \text{ cm}$ ) installed in front of a  $100\times$  (NA = 1.3) oil immersion objective (Zeiss). For the scheme of the

optical setup the reader is referred to the Supporting Information (Figure S1). The resulting intensity at the sample was  $\sim 1 \text{ kW/cm}^2$ . In all experiments the incident laser beam was linearly polarized. Scattered light was collected by the objective, and the Raman fraction was selected using a dichroic mirror and a long-pass filter. The particular set of filters used for each excitation wavelength was as follows: 488 nm, 500DCLP (dichroic), HQ500LP (filter); 532 nm, 540DCLP (dichroic), HQ545LP (filter); 633 nm, R633RDC (dichroic), R633LP (filter); with all optics purchased from Chroma. The Raman scattered light was focused on the entrance of a spectrometer (Acton, 0.15 m) equipped with a 600 g/mm grating and then imaged on a thermoelectrically cooled back-illuminated CCD camera (Princeton Instruments).

We started each experiment by taking an image of the illuminated surface with the grating tuned to zeroth order. Hot spots were identified in such an image (see Results and Discussion). Potential control was then established, and the potential was set at 0.0 V. Tuning the grating back to its first order position, we then registered a series of spectra from each hot spot, while controlling the potential of the working electrode, with the potentiostat and the CCD camera synchronized to each other. Note that SERS spectra were exclusively collected from bright spots of diffraction-limited size, similar to that shown in Figure 1c, by choosing an appropriate region of interest on the CCD chip. The diffraction-limited size of the bright spots was evidently smaller than the size of the Tollens' islands themselves, which could readily be larger than  $\sim 1 \mu\text{m}$ .

Spectra were accumulated during a linear scan in the potential range from 0.0 to  $-1.2 \text{ V}$  and back at a rate of  $9.6 \text{ mV/s}$ . The scan was repeated four times to ensure that the SERS intensity follows the voltage reproducibly, and an overall sequence of 1000 Raman spectra was recorded, with an integration time of 1 s per each. The potential window was selected within the double layer region of the Ag electrode in neutral (pH 7) solutions, so that neither oxidation of Ag nor hydrogen evolution could proceed.<sup>35</sup>

For reference measurements we used  $200 \mu\text{L}$  of a 1 nM water solution of R6G (100 times more diluted than 4MPy). It is important to clarify that the 4MPy and R6G measurements were done separately, so that the two molecules were never coadsorbed on the same surface, during the same experiment. R6G spectra were collected using a 532 nm laser with an intensity of  $100 \text{ W/cm}^2$  at the sample and an integration time of 1 s. All other details were the same as those for 4MPy measurements. We ascertained that photobleaching of the dye molecules did not influence our measurements by taking a series of spectra from each individual R6G molecule (for a sample time series see Supporting Information, Figure S4). The spectra, although fluctuating, were rather stable over a period of several hundreds of seconds. Consequently, R6G

(34) Kirova-Eisner, E.; Bonfil, Y.; Tzur, D.; Gileadi, E. *J. Electroanal. Chem.* **2003**, *552*, 171–183.

(35) Hupp, J. T.; Larkin, D.; Weaver, M. J. *Surf. Sci.* **1983**, *125*, 429–451.

photobleaching does not have an effect on any intensity estimates given below, which were based on individual spectra.

## Results and Discussion

**How many molecules are there in each hot spot?** Images of the ITO surface covered with Tollens' silver islands, taken with the grating at zeroth order, revealed bright spots of size on the order of the diffraction limit (Figure 1c). It is noteworthy that the occurrence of these spots, from which SERS spectra of 4MPy molecules could be registered, was quite rare. Indeed, while the surface was densely covered with silver nanostructures (about six silver clusters within a  $10 \times 10 \mu\text{m}^2$  area; see Figure 1b), in most imaged regions there were no bright spots at all. In some regions we saw one such spot, and the maximum number observed was three. In view of their low density, as well as their diffraction-limited size (smaller than the size of the Tollen's islands themselves, which in many cases were a few micrometers across), these bright spots could be assigned as *individual SERS hot spots*. In fact, we were able to simultaneously observe a silver island using bright field illumination and a hot spot excited by the laser beam. It was evident from these observations (data not shown) that the bright spots were localized on dimensions well below the size of the clusters, and we never saw more than one bright spot per cluster. Thus although there is a possibility that several hot spots were simultaneously excited by the laser in our experiment, it is rather unlikely.

We could also ascertain that the bright spots were due to Raman-scattered light, and not Rayleigh scattering, by observing the color of the scattered light under the microscope (which was redder than the color of the laser), as well as by looking at the full spectrum of this light, which did not show any intensity at  $0 \text{ cm}^{-1}$  (see Supporting Information, Figure S2). Based on the above arguments, we assign the bright spots seen in our data to individual electromagnetic hot spots, as stated above.

But how many 4MPy molecules are there in each of these? We can start with a naïve estimation of the surface coverage of 4MPy, assuming that all molecules were adsorbed. From the analysis of SEM images (Figure 1b), it was found that silver structures cover  $\sim 6\%$  of the geometrical area of the ITO electrode. Consequently, assuming that all 4MPy molecules were adsorbed on the silver surface, the molecular surface density was  $\sim 1 \text{ nm}^{-2}$ . The area of a hot spot could be estimated based on the theoretically predicted enhancement factor distribution of Le Ru et al.<sup>6</sup> Taking the area of each SERS hot spot to be  $\sim 50\text{--}100 \text{ nm}^2$  (it is likely that in silver islands the EM enhancement is also localized in junctions<sup>36</sup>), we find that at most  $\sim 100$  molecules populate each hot spot. Thus even in the extreme case that all molecules are adsorbed on the surface and with the assumption of quite a large hot spot area, there is still only a small number of molecules within the region that provides strong SERS enhancement.

In reality the number of molecules per hot spot must be significantly smaller. Indeed, we have shown in the past that in the case of crystal violet molecules adsorbed on silver nanocrystals, the SERS signal was essentially independent of concentration below  $100 \text{ nM}$ .<sup>37</sup> This indicated that a signal level emanating from not more than one molecule per hot spot was attained already around this concentration, which is similar to

the 4MPy concentration in the current experiment. The fact that only very few hot spots are seen per image also suggests that the actual number of molecules on the surface is much smaller than that obtained from the calculation above, with only one to a few molecules within a hot spot. The reference R6G molecules, which were adsorbed from a solution a hundred times more diluted than that of 4MPy, can definitely be assumed to populate hot spots at the single-molecule level.

**Potential-Dependent SERS Spectra of 4MPy Molecules in Individual Hot Spots.** Typical SERS spectra of 4MPy molecules adsorbed within individual hot spots on Tollens' silver islands, registered at a range of electrode potentials, are shown in Figure 2. The spectra were collected by excitation at 488, 532, and 633 nm. For comparison, in the right panel we show a spectrum of an individual R6G molecule. As noted above, the comparison suggests that the number of molecules in each hot spot is close to the single molecule limit. The spectra are dominated by four pronounced bands at 1013, 1100, 1220, and  $1580 \text{ cm}^{-1}$ . These bands are assigned to modes 1, 12, 9a, and 8a (in the Wilson notation), respectively, which are all totally symmetric.<sup>11,27</sup> While it has been also suggested that the  $1580 \text{ cm}^{-1}$  band might actually be of  $b_2$  symmetry, comparing the above assignment to the recent calculation of Zhao et al.<sup>16</sup> for pyridine on a silver cluster, we believe that the assignment above is more likely. In any case, since both  $a_1$  and  $b_2$  modes are in-plane, none of the following analysis is affected by this issue. The intensities of the four bands are strongly modulated by electrode potential. While other bands of lower intensity are also observed in the spectra, we focus only on these four intense ones. Inspection of the spectra thus provides the following observations: (i) quite a strong signal is obtained from one or a few 4MPy molecules at a fairly modest laser power of  $\sim 1 \text{ kW/cm}^2$ , (ii) all strongly enhanced modes are totally symmetric, (iii) the intensity of all bands increases by a factor of  $\sim 5\text{--}10$  as the voltage is varied from 0 to  $-1.2 \text{ V}$ , and (iv) quite surprisingly, the relative intensities of these bands change as a function of the applied potential, and as a function of excitation wavelength.

**Using R6G To Estimate the Magnitude of Chemical Enhancement of 4MPy.** As was already mentioned in the introduction, SERS of R6G excited at 532 nm involves not only EM enhancement but also additional enhancement due to a molecular resonance. This combination makes SERS from R6G molecules so strong that it can be readily measured at the single-molecule level. The resonance Raman cross sections of various vibrational bands of R6G excited at 532 nm were recently measured by Shim et al.<sup>9</sup> to be  $(0.5\text{--}4) \times 10^{-23} \text{ cm}^2$ . With these known cross sections, R6G molecules adsorbed on a specific surface (i.e., a specific type of hot spot) can serve as a universal reference for estimating the Raman cross sections of other molecules adsorbed on the same surface. Actually the absolute magnitude of the EM enhancement (which is not usually known) becomes unimportant. Of course, to perform such a comparison one also needs to estimate the surface coverage of both reference and target molecules, as well as the incident laser power in each case. However, these details can usually be obtained from experimental parameters, at least roughly, as is the case here. The above discussion assumes that SERS of R6G does not involve any chemical effects. If, as argued by us previously, a CT resonance enhances the SERS of R6G,<sup>38</sup> then the above

(36) Shimada, T.; Imura, K.; Hossain, M. K.; Okamoto, H.; Kitajima, M. *J. Phys. Chem. C* **2008**, *112*, 4033–4035.

(37) Sharaabi, Y.; Shegai, T. O.; Haran, G. *Chem. Phys.* **2005**, *318*, 44–49.

(38) Weiss, A.; Haran, G. *J. Phys. Chem. B* **2001**, *105*, 12348–12354.

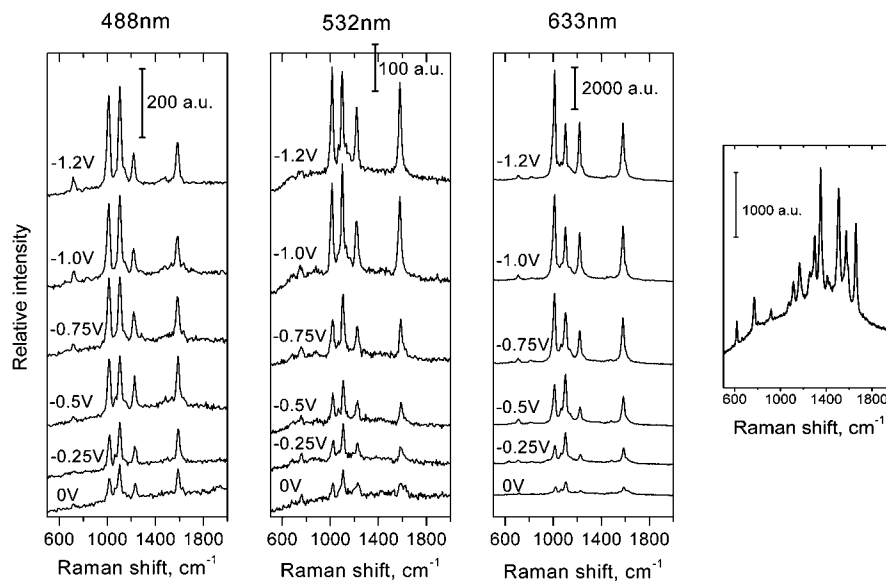


**Figure 2.** Wavelength- and potential-dependent SERS spectra of 4MPy molecules recorded from individual hot spots within Tollens' island structures. At all excitation wavelengths the laser power on the sample was about  $1 \text{ kW/cm}^2$ . For comparison, a SERS spectrum of an individual R6G molecule recorded on Tollens' islands at 532 nm excitation with a laser power of  $100 \text{ W/cm}^2$ , and with no voltage applied, is shown on the right. Vertical bars indicate the signal levels in arbitrary units.

method provides only a lower limit for the unknown Raman cross section.

We now apply the R6G reference method to estimate the Raman cross section of 4MPy. It was argued in the Methods section that each hot spot on the Tollens' island surface contains less than 100 molecules of 4MPy. The spectra of Figure 2 suggest immediately that the observed SERS signals are rather strong, considering that they originate from such a small number of molecules. One should note that the absolute value of the signal varies from hot spot to hot spot, due to various reasons, such as surface heterogeneity. To get an accurate estimate of the ratio between the 4MPy and R6G signals, we collected signals from many hot spots for both molecules. For a proper comparison, one must consider both 4MPy and R6G molecules excited at the same wavelength and at the same electrochemical potential. Since the resonance Raman cross section of R6G is known only for 532 nm excitation,<sup>9</sup> and we have not performed potential dependent studies for this molecule, our choice of experimental parameters was 532 nm excitation and 0 V potential.

Intensity histograms for both the  $1650 \text{ cm}^{-1}$  band of R6G and the  $1580 \text{ cm}^{-1}$  band of 4MPy are shown in the Supporting Information, Figure S3, and average intensities are given in Table S1. Taking into account these average intensities, the differences in numbers of molecules from which the SERS signal originates in each case, as well as differences in laser power (see Methods section), it can be deduced that the SERS cross section of the  $1580 \text{ cm}^{-1}$  band of 4MPy is lower by a factor of  $\sim 3000$  than the cross section of the  $1650 \text{ cm}^{-1}$  band of R6G. Using the value of the resonance Raman cross section of this R6G band,<sup>9</sup> we conclude that the Raman cross section of the strong vibrational bands of 4MPy should be on the order of  $\sigma_{4\text{MPy}} \sim 10^{-26} \text{ cm}^2$ . Thus the Raman cross section of 4MPy is enhanced by at least 3 orders of magnitude in comparison to the nonresonant Raman cross section of similar small organic molecules in solution, such as benzene ( $\sigma_{\text{benzene, free}}^{944\text{cm}^{-1}} \sim 10^{-29} \text{ cm}^2$  at 488 nm excitation<sup>39</sup>).

What can be the origin of an enhancement by a factor of  $10^3$  (or even more in case the number of 4MPy molecules in a hot

spot is in reality smaller than assumed here, or in case the R6G signal is also chemically enhanced, as suggested by us previously<sup>38</sup>)? Since we excite 4MPy far from resonance (the lowest electronic excitation of the molecule is at  $\sim 324 \text{ nm}$ ), we must assign the extra enhancement to a chemical mechanism. As noted in the introduction, there are two types of chemical enhancement. Recently Zhao et al.<sup>16</sup> analyzed computationally the relative contribution of each of these in the case of pyridine adsorbed on a  $\text{Ag}_{20}$  cluster. They found that changes in the static polarizability of the molecule contribute 1 order of magnitude to the enhancement of the Raman signal, while CT resonances enhanced the Raman cross section by  $10^3$ . The latter value can only be a crude estimate, due to the inability of current DFT methodology to properly account for CT interactions.<sup>40</sup> Nevertheless, the comparison of these numbers to our estimate of the chemical enhancement suggests that CT resonances must be active in the case of the SERS of 4MPy as well. To further characterize the contribution of CT resonances, we resorted to potential sweep experiments.

**SERS Spectra under Potential Sweep and the Nature of the CT Resonance.** While sweeping the potential from 0 to  $-1.2 \text{ V}$  and back, we recorded series of SERS spectra from individual hot spots at several excitation wavelengths (see Experimental section). Figure 3 shows intensity oscillations of the  $1013 \text{ cm}^{-1}$  mode extracted from several such series of spectra. Four repetitive potential cycles were performed in each case, showing reproducible behavior. It is seen however that with time the intensity decayed somewhat almost in every trajectory. This is most likely due to modulation of surface structure, as will be discussed below. It is also seen that the trajectories are quite heterogeneous from hot spot to hot spot, in terms of both the maximal amplitude of the signal and the exact voltage where this maximum occurred. This is probably due to local differences in chemical environment around a specific hot spot. In spite of these effects, one can quite easily identify common features

(39) Colles, M. J.; Griffith, J. E. *J. Chem. Phys.* **1972**, *56*, 3384–3391.

(40) Stein, T.; Kronik, L.; Baer, R. *J. Am. Chem. Soc.* **2009**, *131*, 2818–2820.

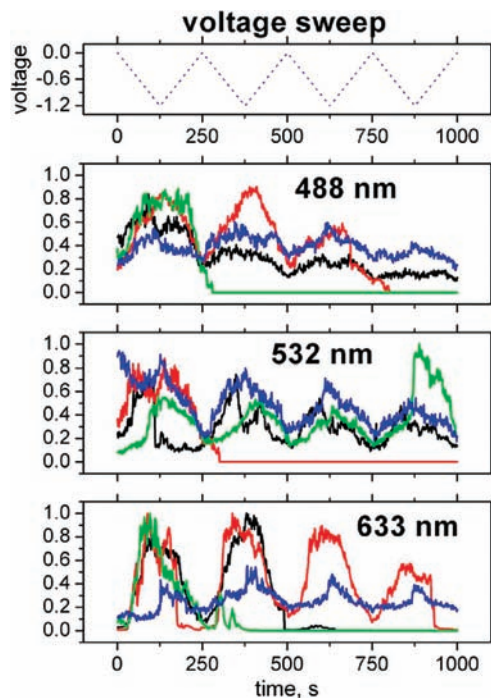


**Figure 3.** Potential sweep experiments performed at various excitation energies. Normalized SERS intensities of the  $1013\text{ cm}^{-1}$  mode of 4MPy molecules, measured from single hot spots at various excitation wavelengths, are shown as a function of time. Each trace represents a particular example of a single hot spot. The upper panel shows the programmed potential sweep as a function of time. Potential-induced SERS intensity oscillations with time are apparent at all three excitation wavelengths. Note that the SERS signal is irreversibly lost in some of the trajectories after one or several cycles.

presented in all trajectories. In particular, the behavior is reversible: SERS intensities tend to increase when the voltage is more negative and drop down when the voltage is tuned back to its most positive values.

Figure 4 shows the normalized SERS intensities of four Raman bands as a function of the applied potential, extracted from the sweep data of Figure 3 and averaged over a few tens of hot spots (33 for 488 nm, 20 for 532 nm, and 22 for 633 nm). During a potential sweep from 0 to  $-1.2\text{ V}$ , the Raman intensities change by a factor of 2–5 depending on the particular normal mode and the excitation wavelength. This change is quite small compared to the overall chemical enhancement of  $10^3$  estimated earlier. As already noted above, there are significant differences in the response curves of different bands. To observe these differences more clearly, Figure 5 presents the ratios between the intensities of the  $1100$ ,  $1220$ , and  $1580\text{ cm}^{-1}$  bands and the intensity of the  $1013\text{ cm}^{-1}$  band. Ratios were first obtained from individual hot spot intensity vs voltage data, similar to those shown in Figure 3, and then averaged over a few tens of hot spots. None of the ratio curves are flat, as might be expected if the response across the spectrum is uniform. Note, however, that the range of energies (or potentials) over which ratios between vibrational bands change is much larger than the largest energy difference between them. We will return to this observation later.

The direction of the CT process can be determined from the dependence of the intensity vs potential response curves on laser frequency. If the peak of the response shifts to more negative potential as the wavelength is tuned to the red, this implies metal-to-molecule CT. This is the case for pyridine<sup>23,24</sup> and *para*-aminothiophenol (PATP)<sup>25</sup> on roughened silver electrodes.

Although it is difficult to discern clear resonance peaks in Figure 4, the wavelength-dependent shift of the curves strongly suggests metal-to-molecule CT. The form of these curves further suggests that the CT resonance is very broad. It is possible that this broad resonance arises from the fact that there is a continuum of very similar states in the conductive band of silver, which can all be involved in the CT transitions.<sup>19</sup>

Lombardi and co-workers<sup>11,21</sup> analyzed CT-associated resonance contributions to SERS. Following Albrecht,<sup>41</sup> they used the Herzberg–Teller theory of vibronic transitions to obtain expressions for the Raman polarizability, including the possibility for electronic transitions which involve CT between the molecule and the metal. For the case of a metal-to-molecule CT transition, two terms are relevant.<sup>11</sup> The A term is operative only in case of resonance of the excitation wavelength with the CT transition. The C term mixes the CT transition (F) with all electronic transitions of the molecule (I), leading to intensity borrowing. It includes Herzberg–Teller coupling terms of the form  $h_{IF} = \langle I | (\partial \hat{H} / \partial Q)_0 | F \rangle$ , where  $(\partial \hat{H} / \partial Q)_0$  is the derivative of the system's Hamiltonian with normal mode Q, evaluated at equilibrium.

The large contribution of the CT resonance to the enhancement of the Raman spectra (at least 3 orders of magnitude), as well as the fact that all strong bands in the spectrum are totally symmetric, suggests that an A-term resonance Raman process is the main contribution to the chemical enhancement. However, the changes in the relative intensities of different vibrational bands of 4MPy with electrode potential, as seen in Figures 4 and 5, cannot be readily explained through the A term. One could imagine that varying the electrode potential leads to sequential tuning into resonance with different vibrational bands. In reality, though, the energetic range over which vibrational ratios change is much larger than the largest energy difference between bands in the Raman spectrum, making this explanation unlikely. Rather, it is possible that tuning the electrode potential affects differently the derivatives of the Hamiltonian with different normal modes. This may lead in turn to a differential effect on different vibronic coupling terms and thus to a change in the relative intensities of different vibrational bands. Thus, vibronic mixing has to be invoked to explain the variations in 4MPy spectra with electrode potential. The involvement of vibronic mixing may also explain why potential tuning leads to a relatively small overall intensity variation, compared to the total chemical enhancement. A detailed investigation of the role of vibronic mixing in potential-dependent Raman spectra of 4MPy is beyond the scope of the current work and might require a thorough theoretical analysis. We point out, however, that, in the case of a metal-to-molecule CT, intensity may be borrowed from the strong plasmon absorption transition of the metallic nanostructure. This is an intriguing possibility, which was not included in the analysis of Lombardi and Birke<sup>11</sup> but is similar in spirit to an early proposal by Lee and Birman.<sup>42</sup> For completion, we note that it is also possible that several CT states are involved in enhancing the Raman scattering of 4MPy molecules on silver, which might also contribute to variations in vibronic mixing.

The results presented above strongly suggest that a CT resonance is responsible for a significant fraction of the enhancement of 4MPy molecules. However, over the years

(41) Tang, J.; Albrecht, A. C. In *Raman Spectroscopy, Theory and Practice*; Szymanski, H. A., Ed.; Plenum: New York, 1970; Vol. 2, pp 33–67.

(42) Lee, T. K.; Birman, J. L. *Phys. Rev. B* **1980**, *22*, 5961–5966.

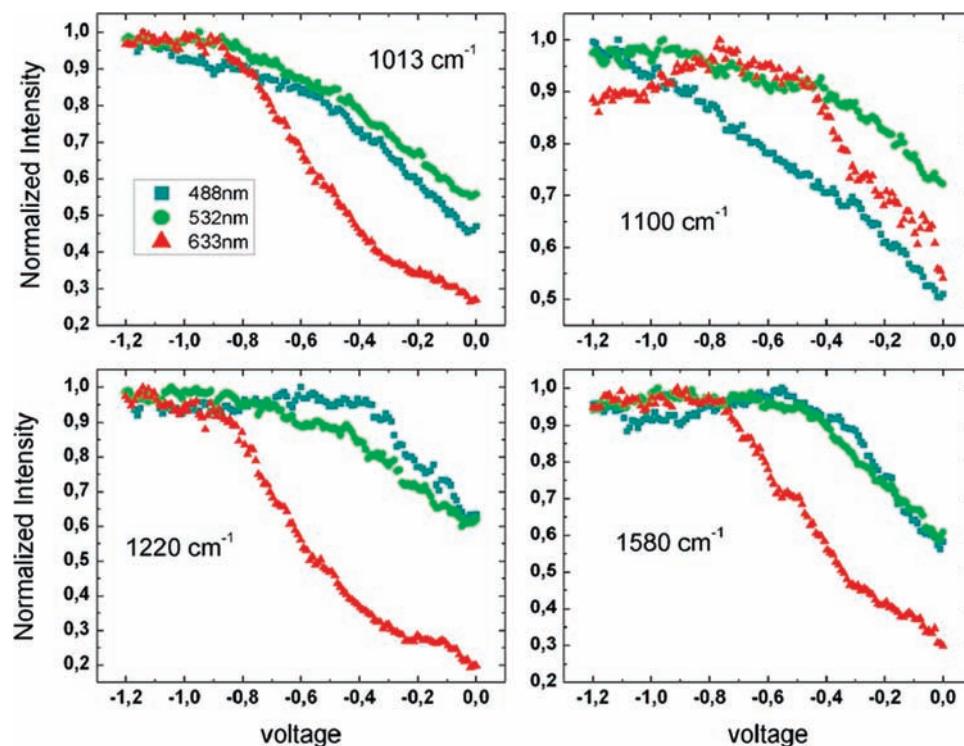


**Figure 4.** Normalized SERS intensity of the four major vibrational modes of 4MPy as a function of applied potential, extracted from the sweep data and averaged over a few tens of hot spots (33 for 488 nm, 20 for 532 nm, and 22 for 633 nm). Different colors represent the three different excitation wavelengths used: cyan, 488 nm; green, 532 nm; and red, 633 nm. The potential at which the SERS signal is maximized is a function of the excitation energy used and the vibrational frequency.

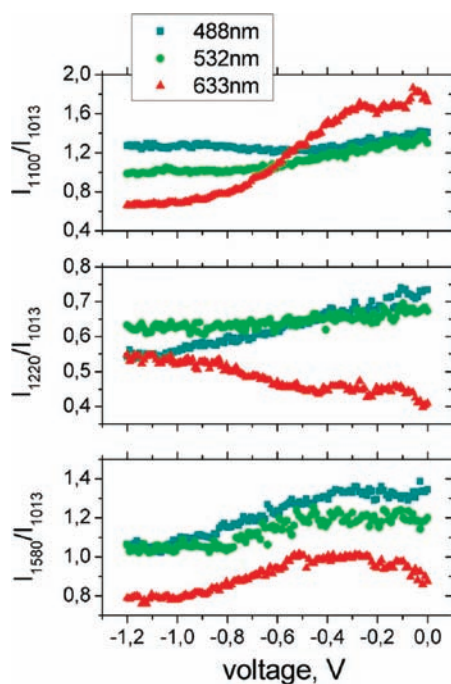


**Figure 5.** Ratios between various 4MPy modes as a function of applied potential and for various excitation wavelengths, obtained from potential sweep experiments similar to those shown in Figure 4 and then averaged over a few tens of hot spots (33 for 488 nm, 20 for 532 nm, and 22 for 633 nm). Color code same as that in Figure 4.

alternative explanations for potential-dependent behavior were raised in the literature. In the following section we discuss such alternatives and discard them.

#### Possible Alternative Causes for Potential-Dependent SERS

**Cross Sections.** It has been suggested that potential-dependent changes in SERS spectra may result from voltage-induced changes in molecular coverage (see e.g. ref 43). Enhanced surface adsorption should lead to increased SERS intensity. While this is a reasonable suggestion in the case of molecules like pyridine, which bind only weakly to the surface and are studied at high concentrations, it is much less likely in the case of a molecule like 4MPy, which not only binds strongly to the surface but also exists in minute concentrations in the solution on top of the silver islands. Further, the changes in relative intensities of vibrational bands of 4MPy (Figure 5) also rule out surface coverage changes, which should affect all vibrational lines uniformly.

A second possibility, which requires a more thorough discussion, is potential-induced molecular reorientation. The intensity of the Raman signal from adsorbate molecules may depend on the molecular orientation with respect to the surface. This is known as the surface selection rule (SSR): essentially only polarizability components in the direction of the local EM (i.e., in a direction perpendicular to the surface) will be enhanced.<sup>44,45</sup> Variation of applied potential under electrochemical conditions can in principle induce reorientation of adsorbed molecules due to modulation of their interaction with the surface and chemical surrounding.<sup>27–30</sup> This should lead to modulation of the spectrum through the SSR.

(43) Kudelski, A.; Bukowska, J. *J. Raman Spectrosc.* **1995**, *26*, 955–958.

(44) Moskovits, M. *J. Chem. Phys.* **1982**, *77*, 4408–4416.

(45) Moskovits, M.; Suh, J. S. *J. Phys. Chem.* **1984**, *88*, 5526–5530.

The molecular orientation of benzenethiol on Au(111) and Ag(111) surfaces was calculated by Bilic et al.<sup>46</sup> It is likely that 4MPy adopts a very similar orientation. It turns out that orientation of benzenethiol on Ag(111) depends on many factors such as the binding site and the surface coverage. Nevertheless, the most stable configuration for diluted coverage was predicted to be one in which the plane of the aromatic ring is somewhat tilted with respect to the surface normal, with an optimal angle of 65°, albeit showing a broad distribution around this angle.

As noted above, all strong bands seen in the SERS spectrum of 4MPy are of  $a_1$  symmetry. By the SSR, these bands should therefore be maximized when the ring is oriented normal to the surface and minimized when the ring is parallel to the surface. Since as the electrode potential is made more negative, the overall intensity of the bands in the spectrum of 4MPy molecules increases, it is possible that the molecules reorient to have their plane aligned more with the normal to the surface. However, in this case out-of-plane modes, e.g. modes of  $a_2$  and  $b_1$  symmetry, should dominate the spectrum in the initial orientation and should then become weaker as the electrode potential is made more negative. In fact, out-of-plane modes are very weakly observed in any of the spectra, if at all. It is therefore unlikely that the increase in the intensity seen in the spectrum is due to reorientation. Rather, it is more reasonable to assume that  $a_1$  bands dominate the spectrum due to a CT resonance. If, as already discussed above, the latter leads to preferential A-term resonance Raman scattering, then only totally symmetric modes will be enhanced.<sup>11</sup> Changes in relative intensities of the observed bands (Figure 5) also do not match a reorientation mechanism.

To summarize, while we cannot completely rule out potential-induced molecular reorientation, we conclude that it cannot account for most of the observed changes in SERS spectra of 4MPy and that a CT resonance must be the major cause for the strong chemical enhancement that we observe. We attribute potential-induced changes in absolute and relative SERS intensities to modulation of the CT cross section, possibly due to changes in vibronic coupling.

**Surface Remodeling under Electrochemical Conditions.** It was pointed out above that the overall intensity of recorded SERS spectra was gradually reduced in consecutive potential sweeps (Figure 3). To find the origin of this phenomenon, we observed the island surfaces under the electron microscope before the experiment and after a few potential sweeps. It was found that the nanoscale roughness of Tollens' islands had essentially vanished following the experiment (Figure S5 of the Supporting Information). Interestingly, such metal surface smoothing appeared uniformly over the whole electrode surface, implying that it was not induced by the laser illumination but rather by electrochemical processes on the electrodes. Clearly, when the surface experiences remodeling like this, its electromagnetic field enhancing ability should vanish.

Jackel et al.<sup>47</sup> have recently reported a related observation. They found out that gold nanobowtie structures, prepared on ITO electrodes and protected by a monolayer of adsorbed *para*-mercaptoaniline molecules, experienced an irreversible process of roughening into "ill-defined" shapes under nonoxidative electrochemical conditions. This process was reflected in

irreversible changes of SERS spectra obtained from these molecules, which appeared already after the first electrochemical cycle. Similarly, it was found by Brus and co-workers that unprotected thermally evaporated silver films on conductive substrates experienced electrochemical Ostwald ripening just minutes after being immersed into pure water.<sup>48</sup>

These findings suggest that roughened or nanostructured electrodes under electrochemical conditions may undergo structural modulations, which should be considered in every experiment. Our sweep experiments allowed us to directly identify changes in SERS signals which are due to such structural modulations. It is not clear to what extent similar structural changes affected observations previously reported in the literature. For example, it could be that irreversible potential-induced spectral changes in SERS spectra of 4MPy<sup>27</sup> and of PATP<sup>25</sup> were due to modification of the electrodes.

## Conclusions

In this work we have focused on the chemical enhancement contribution to SERS of 4MPy molecules adsorbed on Tollens' islands. By comparison to the SERS of the dye R6G, we estimated the chemical enhancement to be  $\sim 10^3$  and attributed it to a CT resonance. In spite of the rather strong chemical enhancement, we found that SERS intensities are affected relatively weakly by an electrode potential in the range of 0 to  $-1.2$  V, for all excitation wavelengths used in this study (488, 532, and 633 nm). This could be an indication of a very broad CT resonance, which may be due to the contribution of conducting electrons below the Fermi level of the metal to the CT transitions.<sup>19</sup> More likely this weak effect on vibrational band intensities is due to changes in vibronic couplings induced by the electrode potential. The charge transfer direction extracted from the comparison between SERS recorded at different excitation wavelengths was determined to be from metal to molecule, in agreement with previous studies for pyridine<sup>23,24</sup> and *para*-aminothiophenol<sup>25</sup> on roughened silver electrodes.

As was already mentioned in the introduction, the study of chemical enhancement in SERS, especially in a quantitative manner, is fraught with difficulties, mainly because of a much stronger EM enhancement. The method discussed here, using a reference molecule, is free of these complications and should be applicable to other molecules. It is especially useful for systems with possible CT excitations which occur in the visible range and consequently naturally overlap with the plasmon resonance. In principle, by simultaneously adsorbing both the reference molecule and the molecule of interest on the same surface, one can further improve the accuracy of this measurement. Indeed, the comparison between contributions of either molecule to the resulting "mixed" signal would be a precise estimate of the Raman cross section for the target molecule.

SERS spectroelectrochemistry close to (or even at) the single-molecule level enabled us to eliminate some of the explanations invoked in the literature for potential-induced intensity variations in SERS spectra and show that CT is indeed the most likely culprit behind these changes. In the future, this kind of spectroscopy is expected to open interesting new research possibilities. In addition to the chemical enhancement mechanism studied here, it should allow studying other types of molecule–electrode charge transfer phenomena with individual molecules. Such studies should facilitate characterization of the

(46) Bilic, A.; Reimers, J. R.; Hush, N. S. *J. Chem. Phys.* **2005**, *122*, 094708.

(47) Jackel, F.; Kinkhabwala, A. A.; Moerner, W. E. *Chem. Phys. Lett.* **2007**, *446*, 339–343.

(48) Redmond, P. L.; Hallock, A. J.; Brus, L. E. *Nano Lett.* **2005**, *5*, 131–135.



heterogeneity in the interaction of molecules with metallic surfaces. They will also enable studying the dynamics of molecule–electrode electron transfer reactions<sup>49</sup> with unprecedented sensitivity.

**Acknowledgment.** G.H. acknowledges the support of the Israel Science Foundation through Grant No. 958/06. A.V. and I.R. acknowledge support of the US–Israel Binational Science Founda-

tion, Grant No. 2004295, and the Minerva Foundation with funding from the Federal German Ministry for Education and Research.

**Supporting Information Available:** Additional figures showing a scheme of the experimental setup, a full-scale spectrum of 4MPy, intensity histograms, a time series of R6G spectra, and Tollen’s islands after repetitive voltage sweeps as well as a table of 4MPy and R6G spectral intensities. This material is available free of charge via the Internet at <http://pubs.acs.org>.

JA904480R

---

(49) Holman, M. W.; Liu, R. C.; Adams, D. M. *J. Am. Chem. Soc.* **2003**, *125*, 12649–12654.